研究论文

DOI：10.11949/0438-1157.

金属掺杂Pt/MFI催化剂对氯乙烯催化氧化活性和选择性的影响研究

徐富文，宋雨纯，王丽，郭耘

（华东理工大学化学与分子工程学院，上海200237）

摘要： 氯乙烯（VC）广泛存在于氯碱工业废气中，其排放危害人类健康和自然环境。金属掺杂沸石骨架可以有效调控催化剂的氧化还原性能和酸碱性，进而影响催化反应性能。本文探讨了金属Al、Ga掺杂对于贵金属Pt负载的纯硅沸石催化剂（Pt/Si-MFI）催化氧化氯乙烯性能的影响，并结合多种表征手段探究了掺杂对于反应影响的机制。金属掺杂一方面增加了催化剂表面酸性、促进了氯乙烯的吸附和活化；另外一方面增加了催化剂表面活性氧物种数量和活性，促进了氯乙烯的进一步氧化；但较多的活性氧物种在高温下也会通过Deacon反应促进Cl_2的生成，导致氯代副产物的形成。该工作揭示了影响氯乙烯氧化活性和氯代副产物选择性的关键因素，为高效催化剂的设计提供了理论支持。

关键词： 氯乙烯；催化氧化；沸石；贵金属催化剂；掺杂

中图分类号： TQ032.4；TQ426.8　　**文献标志码：** AA

文章编号： 0438-1157（XXXX）XX-0001-12

Study on the Effects of Metal Doping on the Activity and Selectivity of Pt/MFI Catalysts for Vinyl Chloride Catalytic Oxidation

XU Fuwen, SONG Yuchun, WANG Li, GUO Yun

(*College of Chemistry and Molecular Engineering, East China University Of Science and Technology, Shanghai* 200237)

Abstract: Vinyl chloride (VC), which is widely present in waste gas from the chlor-alkali industry, is hazardous to human health and the natural environment. Metal doping into the zeolite framework can effectively modulate catalytic performance by regulating the redox properties and surface acidity/basicity of catalysts. Therefore, the effects of Al and Ga doping on the catalytic performance of Pt-supported pure-silica zeolite catalyst (Pt/Si-MFI) for VC oxidation were investigated, and a series of characterization techniques were employed to elucidate the mechanism of metal doping on the reaction. On one hand, metal doping enhances the surface acidity of the catalysts, promoting the adsorption and activation of VC; on the other hand, it increases the amount and reactivity of surface active oxygen species, facilitating the further oxidation of VC. However, excessive active oxygen species at elevated temperatures also favor the formation of Cl_2 via the Deacon reaction, thus promoting the generation of chlorinated by-products. This work reveals the key factors governing the activity of VC and the selectivity of chlorinated by-products, providing theoretical support for the design of high-efficiency catalysts.

Keywords: vinyl chloride; catalytic oxidation; zeolite; noble metal catalyst; doping

收稿日期： 2026-04-16　　**修回日期：** 2026-05-08

通信作者： 王丽（1973—），女，博士，教授，wangli@ecust.edu.cn

第一作者： 徐富文（2001—），男，硕士研究生，15371307075@163.com

基金项目： 国家自然科学基金（22376063）

引用本文： 徐富文, 宋雨纯, 王丽, 郭耘. 金属掺杂Pt/MFI催化剂对氯乙烯催化氧化活性和选择性的影响研究[J]. 化工学报, XXXX, XX(XX): 1-12

Citation: XU Fuwen, SONG Yuchun, WANG Li, GUO Yun. Study on the Effects of Metal Doping on the Activity and Selectivity of Pt/MFI Catalysts for Vinyl Chloride Catalytic Oxidation[J]. CIESC Journal, XXXX, XX(XX): 1-12

引 言

氯乙烯(VC)是一种典型的含氯挥发性有机物(CVOCs),是合成聚氯乙烯(PVC)的重要单体,大量存在于氯碱工业生产的废气中。根据2022年发布的《物质优先清单》中,VC的毒性综合评级高达第四位,仅次于砷、铅、汞。同时,VC也被国际癌症研究机构(IARC)列为一级致癌物,长期接触低浓度的VC会极大地增加患癌风险[1-3]。在不同的CVOCs净化技术中,催化氧化法因效率高、能耗低等优点被认为是目前最有效的CVOCs净化技术之一[4]。

常用于CVOCs催化氧化的催化剂包括贵金属基催化剂、过渡金属基催化剂和沸石基催化剂等。其中,沸石因具有独特的拓扑结构和丰富的酸中心,在CVOCs催化氧化方面受到广泛关注[5-7]。沸石中的酸性位点有利于CVOCs的吸附和活化,而不同的酸种类还会影响氯代副产物的分布。Wang等人[8]发现含有Lewis酸位点的HZSM-5沸石,在三氯乙烯催化氧化中会产生副产物四氯乙烯,而只含有Brønsted酸位点的SBA-15/P沸石上没有四氯乙烯产生。近年来,金属原子掺杂骨架是沸石催化剂设计的关键策略之一,其不仅能够改变沸石的酸性特征,还能调控活性组分的状态。例如,Sn引入沸石骨架会产生Lewis酸位点,从而改变了VC在沸石上的反应路径[9];Ga掺杂进入沸石骨架会引入比Al-MFI更温和的酸性,能够有效抑制副反应以及二次反应的发生[10];Hong等人[11]发现Ge掺杂进入沸石骨架能有效稳定贵金属的状态,抑制其烧结失活。

然而,沸石在CVOCs催化氧化过程中不可避免地会因为积碳和氯沉积而快速失活[12],通过负载过渡金属或者贵金属都可以提高沸石基催化剂的活性和选择性,以实现CVOCs的深度氧化。如在HZSM-5沸石上同时引入Ce和Cr可增加其对于二氯乙烷、二氯甲烷和三氯乙烯的氧化性能[13]。与过渡金属相比,贵金属具有更强的断键的能力和低温活性。Shi等人[14]将Pt引入Ce-USY沸石中,显著促进了氯甲烷和氯乙烯中间物种的深度氧化,从而有效避免了积碳的生成。Su等人[15]研究了Pt、Co和HZSM-5三者的协同作用:酸性位点促进二氯甲烷的吸附和C-Cl键的断裂,Co_3O_4提供充足活性氧并保护Pt免受Cl中毒,Pt则促进中间物种的深度氧化。同样地,Pt和Cr强氧化位点也和ZSM-5沸石存在协同作用,在二氯乙烷催化氧化中表现出优异性能[16]。

综上所述,调控沸石表面的酸性位点的数量和分布有利于CVOCs的吸附活化,而引入贵金属则有利于中间物种的深度氧化,从而抑制积碳失活现象。因此,本文以纯硅Si-MFI沸石为基础,将金属原子(Al和Ga)掺杂进入沸石骨架,以调控MFI沸石的酸强度以及分布。通过进一步负载Pt,探究了金属原子掺杂MFI沸石骨架对于VC催化氧化性能的影响机制。通过多种手段表征分析催化剂的物化性质,并结合原位漫反射红外光谱揭示了VC的反应路径。

1 实验部分

1.1 实验试剂

所有原材料均为AR级,去离子水(H_2O)自制;四丙基氢氧化铵(TPAOH),购自上海笛柏生物科技有限公司;正硅酸四乙酯(TEOS)、氯化钾(KCl),购自上海凌峰化学试剂有限公司;氢氧化钠(NaOH)、硝酸铝($Al(NO_3)_3\cdot 9H_2O$)、硝酸镓($Ga(NO_3)_3\cdot xH_2O$)、醋酸铵(NH_4Ac),购自上海阿拉丁生化科技股份有限公司;四氨合硝酸铂($(NH_3)_4Pt(NO_3)_2$),购自上海阿达玛斯试剂有限公司;N,N-二乙基-1,4-苯二胺(DPD)、乙二胺四乙酸二钠(Na_2EDTA)、磷酸氢二钠(Na_2HPO_4)、磷酸氢二钾(K_2HPO_4)、浓硫酸(H_2SO_4)、硫酸亚铁铵($(NH_4)_2Fe(SO_4)_2$),购自上海麦克林生化科技有限公司。

1.2 催化剂制备

1.2.1 M-MFI载体(M=Si、Al、Ga)的制备 将25.2 g的去离子H_2O和3.2 g的TPAOH(25 wt.%水溶液)混合均匀,缓慢加入8 g的TEOS,室温搅拌2 h,80 ℃搅拌4 h,在此过程中加入0.03 g的NaOH,得到初始凝胶摩尔组成为1 TEOS: 0.1 TPAOH: 0.02 NaOH: 40H_2O的均相溶液。将溶液转移至不锈钢水热釜中,170 ℃水热反应72 h。离心、洗涤、干燥后,550 ℃焙烧4 h,得到Si-MFI沸石。以同样的方法制备Al-MFI和Ga-MFI沸石,区别是在均相溶液中分别加入$Al(NO_3)_3\cdot 9H_2O$和$Ga(NO_3)_3\cdot xH_2O$作为铝源和镓源。将三种载体分别和1M的NH_4Ac离子交换后,离心、干燥、焙烧,得到的固体粉末备用。

1.2.2 Pt/M-MFI催化剂的制备 以$(NH_3)_4Pt(NO_3)_2$为金属前驱体,采用等体积浸渍法将Pt负载在M-MFI沸石上,80 ℃干燥12 h,500 ℃焙烧4 h后,得到

固体粉末备用。

1.3 催化剂表征

X射线衍射实验(XRD)通过Bruke D8Power X-ray Diffraction型X射线衍射仪测得,采用Cu Kα辐射作为入射光源,扫描速度设置为6 °/min;^{29}Si固体核磁实验(^{29}Si NMR)通过BRUKER Avance Ⅲ500 MHz型核磁共振波谱仪测得;氮气低温吸脱附实验通过ASAP 2460型比表面积和孔径吸附仪测得,催化剂样品首先在180 ℃的真空条件下预处理10 h,随后在77.4 K的低温下通入氮气进行吸脱附;电感耦合等离子体发射光谱实验(ICP-OES)通过Agilent 5800 VDV型电感耦合等离子体发射光谱仪测得;高分辨率透射电子显微镜(HRTEM)实验通过ThermoFisher Talos F200X(200 kV)电子显微镜测得;能量色散X射线光谱(EDS-mapping)由SDD Super-X探头执行;氨气程序升温脱附实验(NH_3-TPD)通过PX200装置测得,实验前以40 mL/min的流量通入氩气(Ar)并将样品以10 ℃/min的升温速率升温至400 ℃预处理1 h;吡啶吸附红外实验(Py-IR)通过Thermo Scientific型红外光谱仪测得,实验前在300 ℃真空条件下预处理1 h;氢气程序升温还原实验(H_2-TPR)通过TP-5080装置测得,以商业CuO作为标准样进行测试来定量还原峰面积与H_2消耗量的关系,最后得到催化剂的实际耗氢量;一氧化碳脉冲实验(CO-pulse)和氧气程序升温脱附实验(O_2-TPD)均通过Micromeritics Auto Chem Ⅱ 2920多功能吸附装置测得;X射线光电子能谱实验(XPS)通过Escal.ab 250xi K-Alpha型光电子能谱仪测得;原位漫反射红外实验(In situ DRIFTS)通过Nicolet Nexus 6700型红外光谱仪测得,实验前以50 mL/min的流量通入氩气并将样品以10 ℃/min的升温速率升温至400 ℃预处理1 h。随后以50 ℃为梯度降温至100 ℃,在每个温度点采集背景谱图。然后切换为VC/O_2/Ar混合气,以50 ℃为梯度自100 ℃升温至200 ℃,在每个温度点吸附稳定后采集样品谱图。

1.4 催化剂活性评价

采用固定床石英反应管在常压条件下测试氯乙烯(VC)的催化氧化性能。反应气体由氯乙烯和空气组成(氯乙烯浓度为1000 ppm,反应气体总流速为60 mL/min,反应质量空速(WHSV)为60000 mL·g^{-1}·h^{-1}。氯乙烯及氯代副产物通过气相色谱的氢火焰离子化检测器(FID)进行检测。氯气的选择性通过DPD滴定法测定:采用氢氧化钠溶液吸收各温度点尾气,加入缓冲溶液和DPD溶液变为红色,用硫酸亚铁铵溶液滴定至红色消失。

2 结果与分析

2.1 催化性能评价

载体和催化剂对于氯乙烯(VC)催化氧化的性能曲线如图1(a)所示。载体M-MFI(M=Si, Al, Ga)随着反应温度升高,对于VC氧化的转化率逐渐增加;但在320 ℃时,其对于VC的转化率均低于5 %。贵金属Pt的引入,有效促进了VC的氧化性能,使得Pt/M-MFI对于VC的转化率达到90 %以上。通过提高反应质量空速,在排除内外扩散的影响下(通过提高反应质量空速至120000 mL·g^{-1}·h^{-1},确保反应转化率在2-15 %之间),计算了催化剂在205 ℃时的反应速率(r),列于表1。在该温度下,Pt/Al-MFI的反应速率(267 μmol·g_{pt}^{-1}·s^{-1})高于Pt/Ga-MFI(210 μmol·g_{pt}^{-1}·s^{-1})和Pt/Si-MFI(174 μmol·g_{pt}^{-1}·s^{-1})。考虑到工业废气中水蒸气的存在,因此也评价了催化剂在含水条件下的反应性能。引入5 vol.% H_2O对催化剂活性具有显著促进作用,催化剂的T_{90}均向低温偏移,Pt/Al-MFI和Pt/Ga-MFI均可在400 ℃下实现VC的完全转化。这和H_2O会提供活性羟基或活性氧物种、促进中间物种的快速氧化相关[17]。

为了探究催化剂的稳定性,对催化剂在60000 mL·g^{-1}·h^{-1}、T_{90}温度条件下进行了稳定性测试,如图1(b)所示,在反应最初的7 h内,催化剂均会出现反应性能随着反应时间增加而下降的趋势。比较其下降的程度可以发现Al和Ga的引入提高了催化剂的稳定性,其中Ga的引入对于稳定性的促进作用更显著。

CVOCs催化氧化过程中生成的理想产物为H_2O、CO_2、HCl和Cl_2,但是Cl物种的存在,会导致氯代副产物的生成[4]。催化剂在VC氧化过程中生成的氯代副产物分布如图2(a)所示。当反应温度低于320 ℃时,反应过程中没有检测到氯代副产物。随着反应温度的升高,氯代副产物的浓度随着温度增加呈现“火山型”分布的规律,且催化剂的组成还会影响氯代副产物的分布。在VC氧化过程中,除了生成反/顺-二氯乙烯(E/Z-CHCl=CHCl)外,在Pt/Si-MFI催化VC氧化过程中观察到三氯乙烯(CHCl=

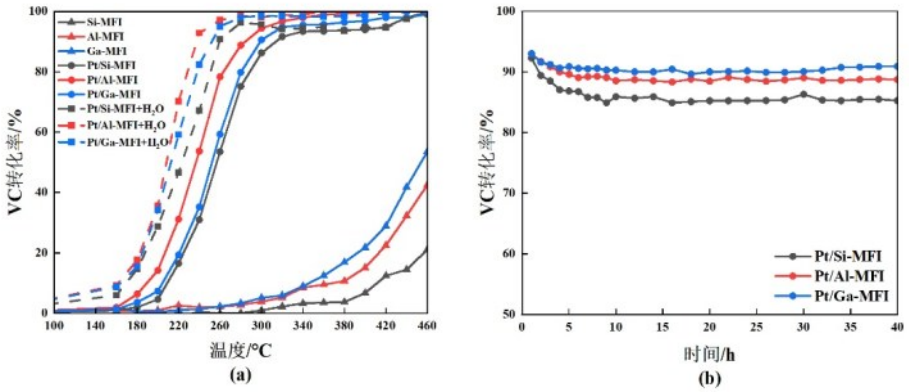

图1　VC催化氧化活性曲线(a)和催化剂的稳定性(b)

Fig. 1　Activity curves for VC catalytic oxidation (a) and Stability of the catalysts (b)

CCl_2)的生成,而在Pt/Al-MFI上还检测到四氯乙烯(CCl_2=CCl_2)的生成。图2(b)为催化剂反应过程中的Cl_2选择性,Pt/Al-MFI催化剂反应过程中Cl_2的选择性高于Pt/Si-MFI和Pt/Ga-MFI,和其具有最多的氯代副产物结果一致。

尾气中多氯乙烯主要由VC多次氯化反应(和Cl_2反应)生成[18],这和Deacon反应($2HCl+1/2O_2 \rightarrow Cl_2+H_2O$)相关,而Deacon反应受温度影响显著,在高温下更有利于反应的发生[19],因此在320 ℃之后Cl_2的选择性显著增加。

有趣的是,在反应气氛中引入5 vol.% H_2O可以有效抑制主要氯代副产物的生成。三种催化剂上均未检测到氯代副产物的生成,这可能是因为H_2O的引入可以去除催化剂表面的Cl物种,从而抑制了氯化反应的发生。

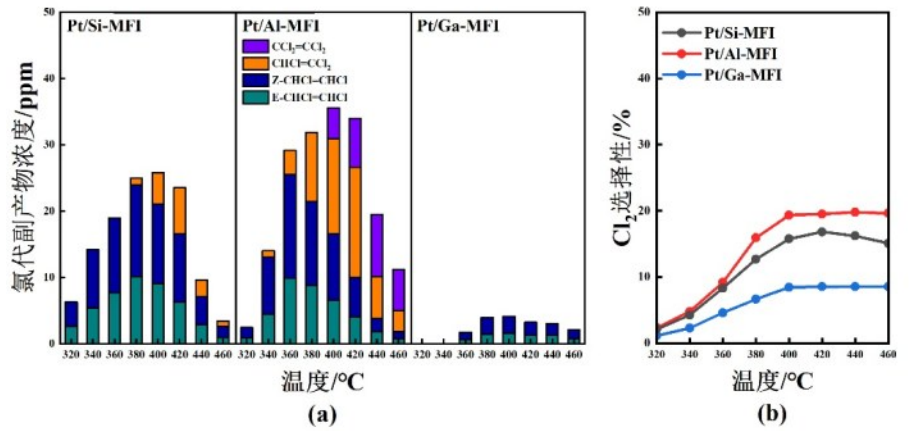

图2　VC催化氧化过程中氯代副产物分布(a)和Cl_2选择性(b)

Fig. 2　Distribution of chlorination by-products (a) and Cl_2 selectivity (b) for VC catalytic oxidation

2.2　催化剂结构表征

表1详细列出了催化剂的结构参数以及催化活性。通过ICP-OES实验测试了反应前后催化剂中Pt的实际含量以及硅和掺杂原子的摩尔比(Si/M),与理论值基本一致,Pt含量在0.4 wt%左右,而Si/Al和Si/Ga分别为64和59;反应后催化剂组成和反应前保持一致。通过N_2低温吸脱附实验测试了Pt/M-MFI催化剂的比表面积(S_{BET}),在沸石骨架中引入金属原子(Al和Ga)对于催化剂的比表面积影响并不显著。

通过XRD对催化剂的晶型结构进行了表征,如图3(a)所示。Pt/M-MFI催化剂在2θ=8 °、8.8 °、23.1 °和24 °出现归属于MFI沸石的典型衍射峰[20-21],未观察到Al_2O_3和Ga_2O_3的衍射峰,这和金属原子(Al和Ga)掺杂进入沸石骨架或掺杂量较小相关。Pt/Al-MFI和Pt/Ga-MFI催化剂的衍射峰强度略低于Pt/Si-MFI催化剂,这是因为金属原子的掺杂导致沸石晶格畸变,增加了结构的无序性[22]。此外,并没有观察到与Pt相关的衍射峰,这可能是因为Pt在沸石上均匀分散或负载量低于检测限。

表1 催化剂的结构参数和催化活性

Table 1 Structural parameters and catalytic activity of the catalysts

催化剂	S_{BET}/(m^2/g)	反应前Si/M	反应后Si/M	Si/M_{fw}	反应前Pt含量/(wt.%)	反应后Pt含量/(wt.%)	Pt分散度①/(%)	r②/(μmol·g_{pt}^{-1}·s^{-1})
Pt/Si-MFI	359	-	-	-	0.40	0.38	87	174
Pt/Al-MFI	337	64	66	72	0.39	0.39	17	267
Pt/Ga-MFI	344	59	59	79	0.42	0.41	19	210

注：①由CO脉冲实验测得②由205 ℃、120000 mL·g^{-1}·h^{-1}空速条件下测得

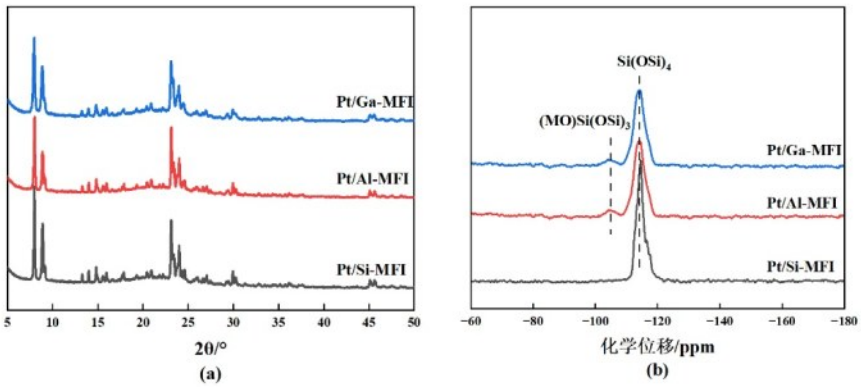

图3 催化剂的XRD谱图(a)和^{29}Si NMR谱图(b)

Fig. 3 XRD patterns (a) and ^{29}Si NMR spectra (b) of the catalysts

采用^{29}Si NMR分析了催化剂中Si原子的化学配位情况，如图3(b)所示。在Pt/Si-MFI催化剂上，仅在-114 ppm处观察到归属于$Si(OSi)_4$物种的特征峰。对于Pt/Al-MFI和Pt/Ga-MFI，除了观察到$Si(OSi)_4$物种外，还观察到位于-104 ppm处归属于$(AlO)Si(OSi)_3$和$(GaO)Si(OSi)_3$物种的振动峰[23]，表明金属原子掺杂进入MFI沸石骨架。MFI沸石骨架中的金属原子比例Si/M_{fw}[24](表1)与ICP测试结果(Si/M)相差不大，可明确Al和Ga主要以Si-O-Al和Si-O-Ga形式存在于MFI沸石骨架中。

图4为催化剂的高分辨率透射电子显微镜(HRTEM)测试结果，从图中可以看出Pt颗粒主要分布于沸石载体的外表面，在沸石骨架中掺杂金属原子(Al和Ga)会影响Pt的分散。Pt/Si-MFI催化剂上Pt颗粒尺寸较小，为1.8 nm。相较于Pt/Si-MFI，Pt/Al-MFI和Pt/Ga-MFI催化剂上Pt颗粒尺寸更大，且两者粒径相近，平均尺寸分别为8.5 nm和7.9 nm。这与利用CO脉冲实验计算的催化剂上Pt的分散度结果一致(表1)。

2.3 催化剂化学性质

通过XPS表征了反应前后催化剂中Pt的化学状态。金属态Pt的Pt $4f_{7/2}$和Pt $4f_{5/2}$轨道分别对应于71.3 eV与74.6 eV处的峰；Pt^{2+}和Pt^{4+}物种的相应峰则分别出现在72.4 eV、75.7 eV和74.3 eV、77.6 eV处[25-26]。反应前Pt/M-MFI催化剂上Pt的价态分布差异明显(图5(a)和表2)，Pt/Si-MFI和Pt/Ga-MFI催化剂主要以Pt^0形式存在，其Pt^0/Pt_{total}比值分别为62.3 %和60.7 %，而Pt/Al-MFI催化剂中氧化态Pt占比更高，Pt^0/Pt_{total}仅为43.4 %。据报道，氧化态Pt更有利于氧的活化[25]，这可能是Pt/Al-MFI表现出较高活性的原因。反应后Pt/M-MFI催化剂主要以Pt^0的形式存在(图5(b)和表2)。反应后Pt/Si-MFI和Pt/Al-MFI的Pt^0/Pt_{total}分别为100 %和74.8 %，这是PtO_x被VC氧化过程中生成的含碳中间物种还原所致[27]；而Pt/Ga-MFI催化剂在反应前后的Pt^0/Pt_{total}比值相近，表明Ga掺杂MFI沸石骨架有利于保持Pt在反应过程中的稳定，这和催化剂稳定性测试结果一致。

通过H_2-TPR研究了催化剂的氧化还原性能，结果如图6(a)所示。51 ℃和175 ℃附近的峰分别归属于沸石表面的PtO和PtO_2的还原[28]，而372 ℃附近的峰则归属于沸石表面与硅醇配位的Pt物种的还原[14]。催化剂中PtO_2还原的理论耗氢量约为41 μmol H_2·g^{-1}，而Pt/M-MFI催化剂的实际耗氢量(表2)均低于理论耗氢量，这与XPS分析结果中催化剂

表面存在金属Pt结果一致。

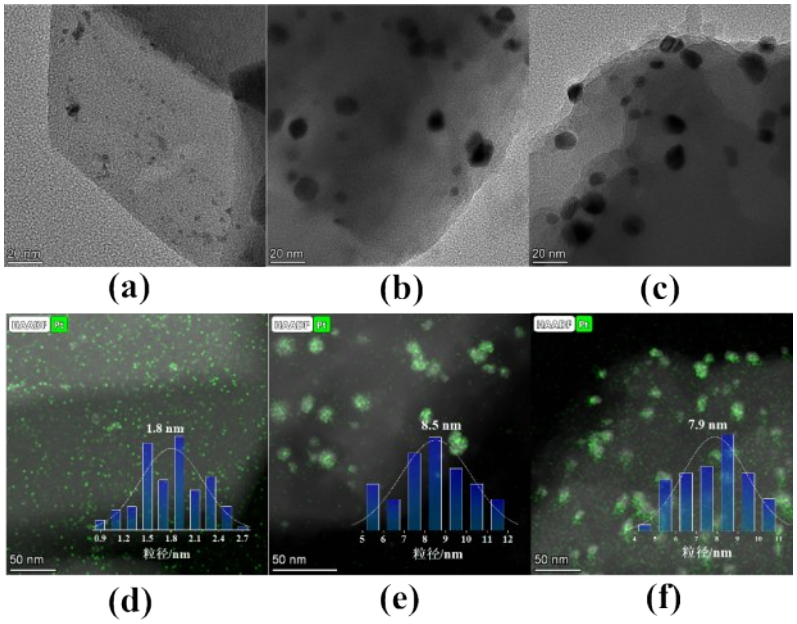

图4　Pt/Si-MFI(a、d)、Pt/Al-MFI(b、e)、Pt/Ga-MFI(c、f)的HRTEM图像和EDS元素映射图

Fig. 4　HRTEM images and EDS elemental mapping images of Pt/Si-MFI (a, d), Pt/Al-MFI (b, e), Pt/Ga-MFI (c, f)

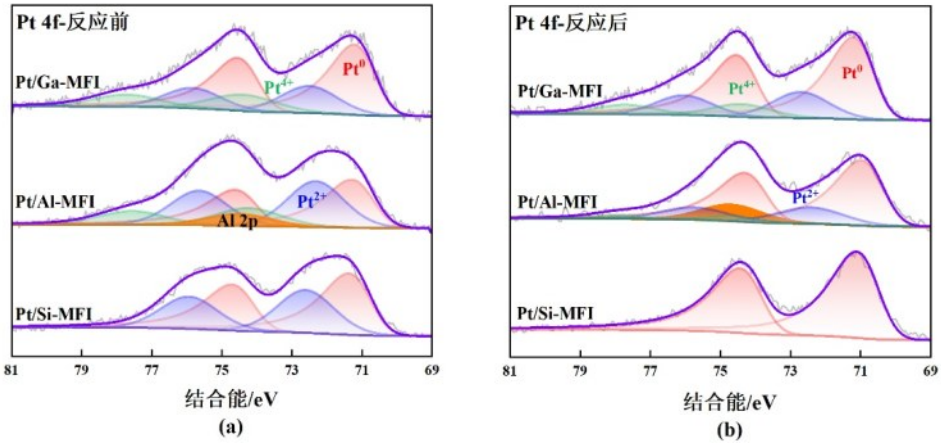

图5　反应前(a)和反应后(b)催化剂的Pt 4f XPS谱图

Fig. 5　Pt 4f XPS spectra of fresh catalysts (a) and used catalysts (b)

通过O_2-TPD进一步表征了催化剂表面氧物种的状态，结果如图6(b)所示。低于200 ℃的峰与物理吸附氧的脱附有关，而400 ℃以上的峰归属于表面晶格氧的脱附[29]。相比于Pt/Si-MFI，Al和Ga的掺杂增加了催化剂对于氧活化的能力，表现在表面晶格氧的脱附温度向低温偏移以及峰面积的增加。以Pt/Al-MFI的O_2脱附峰面积为1.00，根据峰面积积分计算了催化剂上O_2脱附峰的相对面积(表2)。考虑到低于200 ℃时VC的反应性能较差，较高温度脱附的氧(表面晶格氧)对反应性能的影响更显著。此外，催化剂表面的活性氧物种在高温下更有利于Deacon反应的发生[30~32]，提高了尾气中Cl_2的选择性，从而导致氯代副产物的生成。

酸性位点在CVOCs催化氧化过程中具有重要作用，其强度、数量与种类会影响反应物吸附活化、中间物种转化路径以及最终产物分布[8~9,19]。通过NH_3-TPD测试了催化剂在反应前后的表面酸性，如图7所示。100-250 ℃的峰归属于吸附在弱酸位点上NH_3的脱附，而250-400 ℃的峰则归属于NH_3在强酸位点的脱附[33]。新鲜Pt/Si-MFI未观察到明显的NH_3的脱附峰，表明Pt/Si-MFI基本不具有酸性；而在Pt/Al-MFI和Pt/Ga-MFI表面则同时存在强酸

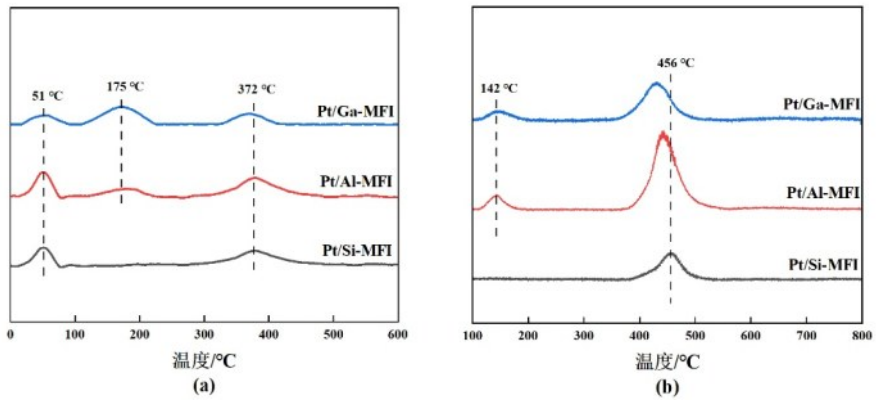

图6 催化剂的H_2-TPR(a)和O_2-TPD(b)谱图

Fig. 6 H_2-TPR (a) and O_2-TPD (b) profiles of the catalysts.

表2 催化剂的化学状态和氧化性能

Table 2 Chemical state and oxidation ability of the catalysts

催化剂	反应前 Pt^0/Pt_{total}/(%)	反应后 Pt^0/Pt_{total}/(%)	实际耗氢量/(μmol $H_2\cdot g^{-1}$)	O_2相对脱附峰面积
Pt/Si-MFI	62.3	100	10.1	0.34
Pt/Al-MFI	43.4	74.8	15.8	1.00
Pt/Ga-MFI	60.7	67.6	12.2	0.55

和弱酸位点。与Pt/Al-MFI相比,Pt/Ga-MFI沸石上NH_3脱附峰向低温偏移,这是因为Si和Al之间的电负性差异大于Si和Ga,使得Si-OH-Al的酸性强度高于Si-OH-Ga[34-36]。催化剂表面酸量和NH_3脱附峰面积成正比,以新鲜Pt/Al-MFI的脱附峰面积为1.00,获得催化剂酸量的相对大小。由表3可知,Pt/Al-MFI和Pt/Ga-MFI催化剂的强酸/总酸比例以及表面酸量在反应前后变化不显著,这是因为氧化过程中氯乙烯中的H原子或者反应生成的H_2O会补充沸石消耗的羟基位点[37-38]。结合新鲜和使用后催化剂在不同温度范围内NH_3脱附温度相近以及脱附峰面积的变化,表明氯乙烯氧化后未影响催化剂表面的酸性。

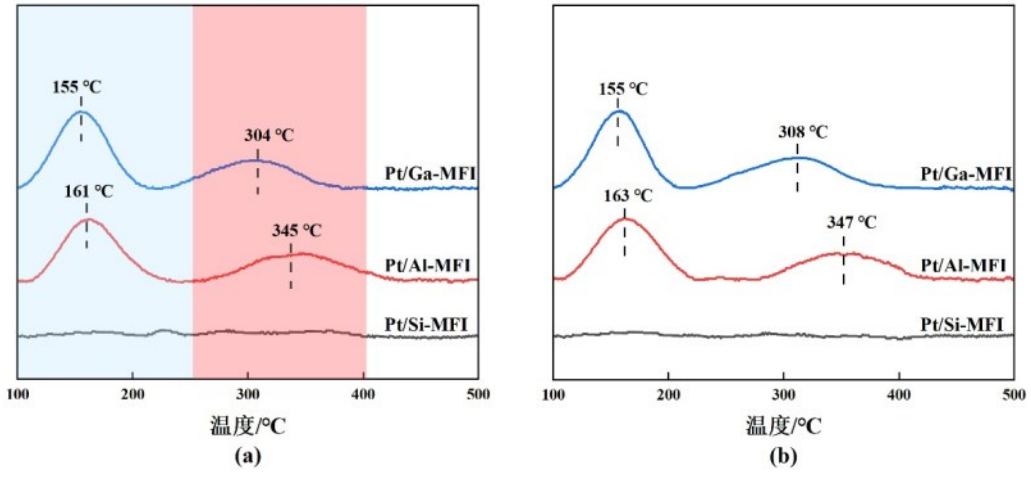

图7 反应前(a)和反应后(b)催化剂的NH_3-TPD谱图

Fig. 7 NH_3-TPD profiles of fresh catalysts (a) and used catalysts (b)

Brønsted酸位点有利于CVOCs的吸附活化,而Lewis酸位点有利于C-Cl键的解离[39],因此通过吡啶吸附红外技术探究了催化剂表面的酸分布,如图8(a)所示。1543 cm^{-1}和1455 cm^{-1}处的特征峰分别

可归属于吡啶在Brønsted酸位点上的吸附(PyH^+)和在Lewis酸位点的吸附(PyL)[36,40]。Pt/Si-MFI催化剂表面仅观察到微弱的吡啶吸附峰,表明催化剂表面酸中心较少,与NH_3-TPD结果一致。Pt/Al-MFI和Pt/Ga-MFI催化剂表面同时存在Brønsted和Lewis酸位点。从吡啶吸附峰强度可知,Pt/Al-MFI和Pt/Ga-MFI主要以Brønsted酸位点为主。Pt/Al-MFI的总酸量(208 μmol·g^{-1})和Pt/Ga-MFI(216 μmol·g^{-1})相近,但是催化剂表面Brønsted酸和Lewis酸的分布不同(表3)。Pt/Al-MFI表面Brønsted酸和Lewis酸比值(B/L)为16.8,高于Pt/Ga-MFI(9.2)。

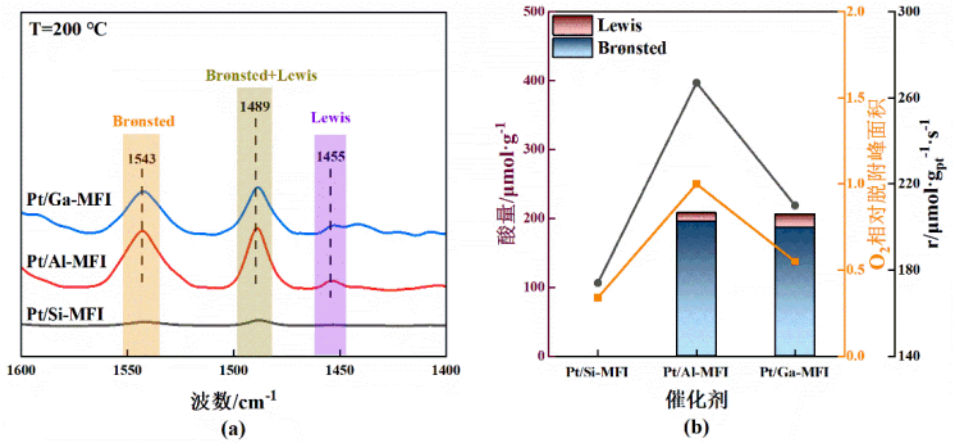

图8　催化剂的吡啶吸附红外谱图(a);酸量、氧化能力和反应速率的关系(b)

Fig. 8　Py-IR spectra of the catalysts (a); Relationship among acidity, oxidation capacity and reaction rate (b)

将催化剂表面酸量、活性氧数量与反应速率结果汇总,如图8(b)所示。Pt/Si-MFI酸性弱,即便活性氧物种数量与Pt/Ga-MFI相近,但其反应速率(174 μmol·g_{pt}^{-1}·s^{-1})低于Pt/Ga-MFI(210 μmol·g_{pt}^{-1}·s^{-1});而Pt/Al-MFI与Pt/Ga-MFI酸性相近,但前者拥有更多的活性氧物种,因此具有最高的反应速率(267 μmol·g_{pt}^{-1}·s^{-1})。上述结果表明,酸性位点和活性氧物种会显著影响Pt/M-MFI催化剂的催化性能。

表3　催化剂的酸性

Table 3　Acidity of the catalysts

催化剂	反应前 相对酸量	反应后 相对酸量	反应前 强酸/总酸	反应后 强酸/总酸	总酸量①/ (μmol·g^{-1})	B/L
Pt/Si-MFI	–	–	–	–	–	–
Pt/Al-MFI	1.00	1.03	0.42	0.45	208	16.8
Pt/Ga-MFI	1.05	1.07	0.36	0.37	216	9.2

注:①由200 ℃下吡啶吸附红外实验测得

2.4　反应机理分析

通过原位漫反射红外实验探讨了Pt/Si-MFI和Pt/Al-MFI催化剂上VC的吸附和反应机理,结果如图9所示。3500-3800 cm^{-1}为羟基伸缩振动特征峰:3743 cm^{-1}处的峰归属于末端孤立Si-OH,3660 cm^{-1}处的峰归属于MFI骨架外铝物种的Al-OH,而3606 cm^{-1}处的峰则归属于桥连的Si-OH[18]。在3087 cm^{-1}处的峰来自烯烃上的C-H键的振动,而1605 cm^{-1}处出现的强峰则属于VC上的C=C键的弯曲振动[41]。

在100 ℃下,VC在Pt/Si-MFI表面吸附5 min时可观察到VC吸附的特征峰(1605 cm^{-1}),吸附时间增加至30 min,VC吸附峰强度亦随之增强。在该温度下引入O_2之后,未观察到有反应中间物种的生成。反应温度增加到150 ℃,在1700 cm^{-1}和2110 cm^{-1}处分别观察到归属于羧酸的C=O振动峰[42]以及CO在Pt上的吸附特征峰[43],这是VC氧化生成的反应中间物种。200 ℃时催化剂表面羧酸的特征峰增强表明该物种在催化剂表面积累。

相比之下,VC在Pt/Al-MFI表面吸附过程中,除了观察到VC吸附峰外,还观察到羟基的消耗峰(3606 cm^{-1})、CO的吸附峰(2096 cm^{-1})以及归属于醛的C=O振动峰(1740 cm^{-1})[44-45],这是由于VC被Pt/

Al-MFI催化剂表面的活性氧物种氧化所致，表明Pt/Al-MFI比Pt/Si-MFI具有更强的氧化能力。通入O_2升温之后，羟基消耗峰、CO以及醛的特征峰迅速消失，说明O_2的加入促进了活性氧物种的补充，有利于CO和醛的氧化。Pt/Al-MFI表面同样出现了羧酸的积累，表明羧酸的进一步氧化为反应的速控步骤。

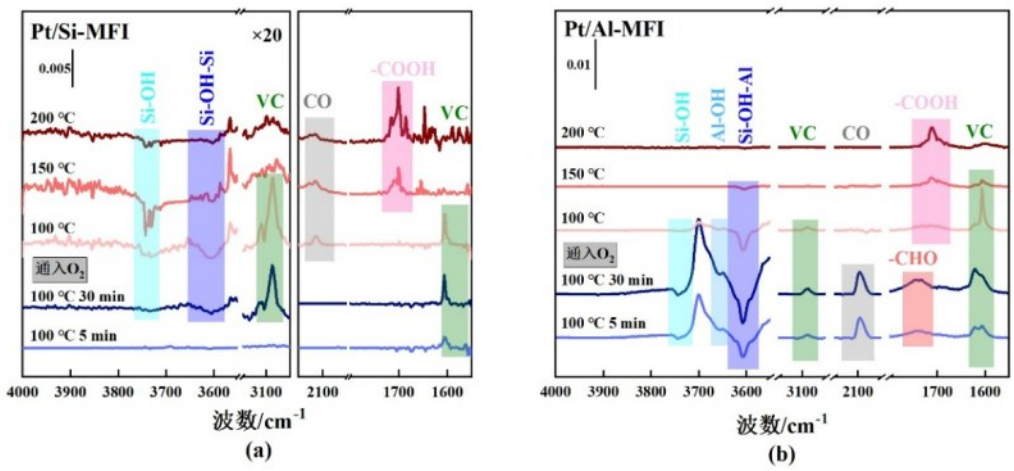

图9 Pt/Si-MFI(a)和Pt/Al-MFI(b)的VC吸附/氧化原位红外光谱

Fig. 9 In situ DRIFTS spectra of VC adsorption/oxidation over Pt/Si-MFI (a) and Pt/Al-MFI (b)

根据原位漫反射红外实验结果，我们提出了Pt/Si-MFI和Pt/Al-MFI催化剂上VC氧化的反应机理，如图10所示。首先，氯乙烯优先吸附在酸性位点上，活性氧物种进攻C-Cl键生成醛，随后转化为羧酸，最终被氧化为CO_2和H_2O。相对于Pt/Si-MFI催化剂，Pt/Al-MFI表面丰富的酸性位点有利于氯乙烯的吸附活化，而活性氧物种则可以促进氯乙烯的进一步氧化。

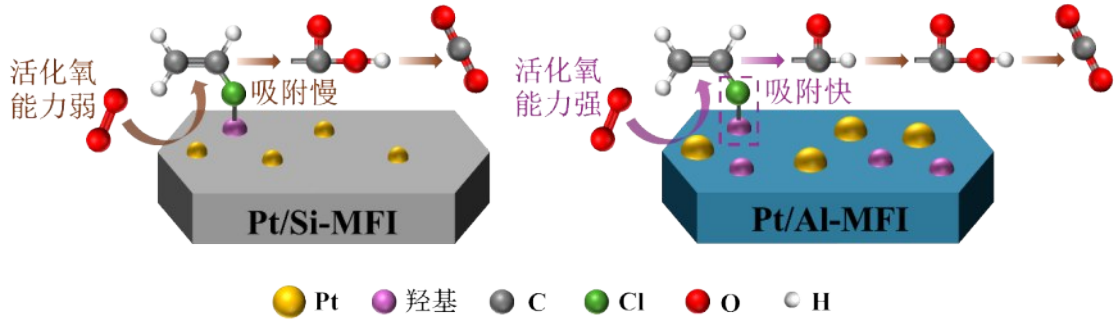

图10 催化剂上VC氧化的反应机理

Fig. 10 Reaction mechanism for VC oxidation over the catalysts

3 结论

本文通过水热法成功制备了Pt/M-MFI催化剂(M=Si、Al、Ga)，探究了金属原子(Al和Ga)掺杂沸石骨架对于催化剂催化氧化氯乙烯性能的影响。Al掺杂催化剂(Pt/Al-MFI)可有效提高氯乙烯的反应速率，在205 ℃时的反应速率是未掺杂催化剂(Pt/Si-MFI)的1.5倍；而Ga的引入还可以有效抑制催化剂在高温下多氯代副产物的生成、提高催化剂的稳定性。反应气氛中水的存在可以进一步提高氯乙烯的氧化性能，使得Pt/Al-MFI催化剂的T_{90}仅为238 ℃，并有效抑制氯代副产物生成。金属掺杂沸石骨架虽然抑制了Pt的分散，但却有效增加了催化剂的酸性和氧化还原性能，从而促进氯乙烯在低温下的吸附和进一步氧化，使得氯乙烯全转化温度向低温偏移；但较多的活性氧物种在高温下也会有利于氯化反应的发生，从而导致氯代副产物的生成。

参考文献

[1] Wang C, Zhang C H, Hua W C, et al. Catalytic Oxidation of Vinyl Chloride Emissions over Co-Ce Composite Oxide Catalysts[J]. Chemical Engineering Journal, 2017.
Wang C, Zhang C H, Hua W C, et al. Catalytic oxidation of vinyl chloride emissions over Co-Ce composite oxide catalysts[J]. Chemical Engineering Journal, 2017, **315**: 392-402.[LinkOut]

[2] Agency for Toxic Substances and Disease Registry. Substance Priority List[EB/OL]. Atlanta: ATSDR, [2026-04-15]. https://www.atsdr.cdc.gov/programs/substance-priority-list.html.
网址有效. 点击这里, 可链出核对其他内容

[3] Lorenzo T. IARC Monographs on the Evaluation of Carcinogenic Risks to Humans: Volume 100F[M]. Lyon: International Agency for Research on Cancer, 2012: 451-473.【自助补缺】【自助补缺】【自助补缺】【自助补缺】

[4] Lin F W, Zhang Z M, Li N, et al. How to Achieve Complete Elimination of Cl-VOCs: A Critical Review on Byproducts Formation and Inhibition Strategies during Catalytic Oxidation[J]. Chemical Engineering Journal, 2021, **404**: 126534.
Lin F W, Zhang Z M, Li N, et al. How to achieve complete elimination of Cl-VOCs: a critical review on byproducts formation and inhibition strategies during catalytic oxidation[J]. Chemical Engineering Journal, 2021, **404**: 126534.[LinkOut]

[5] López-Fonseca R, Aranzabal A, Gutiérrez-Ortiz J I, et al. Comparative Study of the Oxidative Decomposition of Trichloroethylene over H-Type Zeolites under Dry and Humid Conditions[J]. Applied Catalysis B: Environmental, 2001, **30**(3-4): 303-313.
López-Fonseca R, Aranzabal A, Gutiérrez-Ortiz J I, et al. Comparative study of the oxidative decomposition of trichloroethylene over H-type zeolites under dry and humid conditions[J]. Applied Catalysis B: Environmental, 2001, **30**(3/4): 303-313.[LinkOut]

[6] López-Fonseca R, Aranzabal A, Steltenpohl P, et al. Performance of Zeolites and Product Selectivity in the Gas-Phase Oxidation of 1,2-Dichloroethane[J]. Catalysis Today, 2000, **62**(4): 367-377.
López-Fonseca R, Aranzabal A, Steltenpohl P, et al. Performance of zeolites and product selectivity in the gas-phase oxidation of 1, 2-dichloroethane[J]. Catalysis Today, 2000, **62**(4): 367-377.[LinkOut]

[7] López-Fonseca R, Cibrián S, Gutiérrez-Ortiz J I, et al. Oxidative Destruction of Dichloromethane over Protonic Zeolites[J]. AIChE Journal, 2003, **49**(2): 496-504.
López-Fonseca R, Cibrián S, Gutiérrez-Ortiz J I, et al. Oxidative destruction of dichloromethane over protonic zeolites[J]. AIChE Journal, 2003, **49**(2): 496-504.[LinkOut]

[8] Wang T T, Dai Q G, Yan F W. Effect of Acid Sites on Catalytic Destruction of Trichloroethylene over Solid Acid Catalysts[J]. Korean Journal of Chemical Engineering, 2017, **34**(3): 664-671.
Wang T T, Dai Q G, Yan F W. Effect of acid sites on catalytic destruction of trichloroethylene over solid acid catalysts[J]. Korean Journal of Chemical Engineering, 2017, **34**(3): 664-671.[LinkOut]

[9] Li M Q, Cai Y A, Zhan W C, et al. Revealing the Effect of Framework Acidity on the Catalytic Combustion of Vinyl Chloride over Zeolite-Based Catalysts[J]. Separation and Purification Technology, 2024, **340**: 126773.
Li M Q, Cai Y A, Zhan W C, et al. Revealing the effect of framework acidity on the catalytic combustion of vinyl chloride over zeolite-based catalysts[J]. Separation and Purification Technology, 2024, **340**: 126773.[LinkOut]

[10] Mentzel U V, Højholt K T, Holm M S, et al. Conversion of Methanol to Hydrocarbons over Conventional and Mesoporous H-ZSM-5 and H-Ga-MFI: Major Differences in Deactivation Behavior[J]. Applied Catalysis A: General, 2012, **417-418**: 290-297.
Mentzel U V, Højholt K T, Holm M S, et al. Conversion of methanol to hydrocarbons over conventional and mesoporous H-ZSM-5 and H-Ga-MFI: Major differences in deactivation behavior[J]. Applied Catalysis A: General, 2012, **417**: 290-297.[LinkOut]

[11] Hong H Z, Xu Z K, Mei B B, et al. A Self-Regenerating Pt/Ge-MFI Zeolite for Propane Dehydrogenation with High Endurance [J]. Science, 2025, **388**(6746): 497-502.
Hong H Z, Xu Z K, Mei B B, et al. A self-regenerating Pt/Ge-MFI zeolite for propane dehydrogenation with high endurance[J]. Science, 2025, **388**(6746): 497-502.[LinkOut]

[12] Aranzabal A, González-Marcos J A, Romero-Sáez M, et al. Stability of Protonic Zeolites in the Catalytic Oxidation of Chlorinated VOCs (1,2-Dichloroethane)[J]. Applied Catalysis B: Environmental, 2009, **88**(3-4): 533-541.
Aranzabal A, González-Marcos J A, Romero-Sáez M, et al. Stability of protonic zeolites in the catalytic oxidation of chlorinated VOCs (1, 2-dichloroethane)[J]. Applied Catalysis B: Environmental, 2009, **88**(3/4): 533-541.[LinkOut]

[13] Yang P, Xue X M, Meng Z H, et al. Enhanced Catalytic Activity and Stability of Ce Doping on Cr Supported HZSM-5 Catalysts for Deep Oxidation of Chlorinated Volatile Organic Compounds[J]. Chemical Engineering Journal, 2013, **234**: 203-210.
Yang P, Xue X M, Meng Z H, et al. Enhanced catalytic activity and stability of Ce doping on Cr supported HZSM-5 catalysts for deep oxidation of chlorinated volatile organic compounds[J]. Chemical Engineering Journal, 2013, **234**: 203-210.[LinkOut]

[14] Shi Y J, Li Z M, Wang J L, et al. Synergistic Effect of Pt/Ce and USY Zeolite in Pt-Based Catalysts with High Activity for VOCs Degradation[J]. Applied Catalysis B: Environmental, 2021, **286**: 119936.
Shi Y J, Li Z M, Wang J L, et al. Synergistic effect of Pt/Ce and USY zeolite in Pt-based catalysts with high activity for VOCs degradation[J]. Applied Catalysis B: Environmental, 2021, **286**: 119936.[LinkOut]

[15] Su Y, Fu K X, Zheng Y F, et al. Catalytic Oxidation of Dichloromethane over Pt-Co/HZSM-5 Catalyst: Synergistic Effect of Single-Atom Pt, Co_3O_4, and HZSM-5[J]. Applied Catalysis B: Environmental, 2021, **288**: 119980.
Su Y, Fu K X, Zheng Y F, et al. Catalytic oxidation of dichloromethane over Pt-Co/HZSM-5 catalyst: Synergistic effect of single-atom Pt, Co_3O_4, and HZSM-5[J]. Applied Catalysis B: Environmental, 2021, **288**: 119980.[LinkOut]

[16] Shi Y J, Wang J L, Wang Y Y, et al. Synergistic Effect in Bimetal Cr-Pt/ZSM-5 Catalysts with High Activity for CVOCs Low-Temperature Removal[J]. Journal of Environmental Chemical

Engineering, 2022, **10**(3): 107629.
Shi Y J, Wang J L, Wang Y Y, et al. Synergistic effect in bimetal Cr-Pt/ZSM-5 catalysts with high activity for CVOCs low-temperature removal[J]. Journal of Environmental Chemical Engineering, 2022, **10**(3): 107629.[LinkOut]

[17] Lv X L, Wu S N, Shao S T, et al. Efficient Catalytic Elimination of Chlorobenzene Based on the Water Vapor-Promoting Effect within Mn-Based Catalysts: Activity Enhancement and Polychlorinated Byproduct Inhibition[J]. Environmental Science & Technology, 2024, **58**(8): 3985-3996.
Lv X L, Wu S N, Shao S T, et al. Efficient catalytic elimination of chlorobenzene based on the water vapor-promoting effect within Mn-based catalysts: activity enhancement and polychlorinated byproduct inhibition[J]. Environmental Science & Technology, 2024, **58**(8): 3985-3996.[LinkOut]

[18] Wang H, Peng B, Zhang R D, et al. Synergies of Mn Oxidative Ability and ZSM-5 Acidity for 1, 2-Dichloroethane Catalytic Elimination[J]. Applied Catalysis B: Environmental, 2020, **276**: 118922.
Wang H, Peng B, Zhang R D, et al. Synergies of Mn oxidative ability and ZSM-5 acidity for 1, 2-dichloroethane catalytic elimination[J]. Applied Catalysis B: Environmental, 2020, **276**: 118922.[LinkOut]

[19] Gołąbek K, Palomares A E, Martínez-Triguero J, et al. Ce-Modified Zeolite BEA Catalysts for the Trichloroethylene Oxidation. The Role of the Different and Necessary Active Sites [J]. Applied Catalysis B: Environmental, 2019, **259**: 118022.
Gołąbek K, Palomares A E, Martínez-Triguero J, et al. Ce-modified zeolite BEA catalysts for the trichloroethylene oxidation. The role of the different and necessary active sites[J]. Applied Catalysis B: Environmental, 2019, **259**: 118022.[LinkOut]

[20] Wang S F, Wang Y H, Chu P Q, et al. Glycerol-Modified Ce-Co Catalysts for Efficient Degradation of Dichloromethane: Physicochemical Properties and Reaction Pathways[J]. Journal of Environmental Chemical Engineering, 2023, **11**(3): 109811.
Wang S F, Wang Y H, Chu P Q, et al. Glycerol-modified Ce-Co catalysts for efficient degradation of dichloromethane: Physicochemical properties and reaction pathways[J]. Journal of Environmental Chemical Engineering, 2023, **11**(3): 109811.[LinkOut]

[21] Yuan E H, Dai W L, Wu G J, et al. Facile Synthesis of Sn-Containing MFI Zeolites as Versatile Solid Acid Catalysts[J]. Microporous and Mesoporous Materials, 2018, **270**: 265-273.
Yuan E H, Dai W L, Wu G J, et al. Facile synthesis of Sn-containing MFI zeolites as versatile solid acid catalysts[J]. Microporous and Mesoporous Materials, 2018, **270**: 265-273.[LinkOut]

[22] Mediavilla M, Melo L, Díaz Y, et al. Influence of the Acid Sites Density in the Acetone Transformation over Bifunctional Pt/H[Ga] ZSM5 Catalysts[J]. Microporous and Mesoporous Materials, 2007, **102**(1-3): 86-94.
Mediavilla M, Melo L, Díaz Y, et al. Influence of the acid sites density in the acetone transformation over bifunctional Pt/H [Ga] ZSM5 catalysts[J]. Microporous and Mesoporous Materials, 2007, **102**(1/2/3): 86-94.[LinkOut]

[23] Leth K T, Rovik A K, Holm M S, et al. Synthesis and Characterization of Conventional and Mesoporous Ga-MFI for Ethane Dehydrogenation[J]. Applied Catalysis A: General, 2008, **348**(2): 257-265.
Leth K T, Rovik A K, Holm M S, et al. Synthesis and characterization of conventional and mesoporous Ga-MFI for ethane dehydrogenation[J]. Applied Catalysis A: General, 2008, **348**(2): 257-265.[LinkOut]

[24] Bradley S M, Howe R F, Kydd R A. Correlation between ^{27}Al and ^{71}Ga NMR Chemical Shifts[J]. Magnetic Resonance in Chemistry, 1993, **31**(10): 883-886.
Bradley S M, Howe R F, Kydd R A. Correlation between ^{27}Al and ^{71}Ga NMR chemical shifts[J]. Magnetic Resonance in Chemistry, 1993, **31**(10): 883-886.[LinkOut]

[25] Shi Y J, Kong F Z, Wan J, et al. Synergistic Effect of ZSM-5 Zeolite in Pt-CeO_2-TiO_2/ZSM-5 Catalysts for Highly Efficient Catalytic Oxidation of VOCs[J]. Industrial & Engineering Chemistry Research, 2023, **62**(8): 3546-3556.
Shi Y J, Kong F Z, Wan J, et al. Synergistic effect of ZSM-5 zeolite in Pt - CeO_2 - TiO_2/ZSM-5 catalysts for highly efficient catalytic oxidation of VOCs[J]. Industrial & Engineering Chemistry Research, 2023, **62**(8): 3546-3556.[LinkOut]

[26] Li Z Y, Gao R Y, Hou Z Q, et al. Tandem Supported Pt and ZSM-5 Catalyst with Separated Catalytic Functions for Promoting Multicomponent VOCs Oxidation[J]. Applied Catalysis B: Environmental, 2023, **339**: 123131.
Li Z Y, Gao R Y, Hou Z Q, et al. Tandem supported Pt and ZSM-5 catalyst with separated catalytic functions for promoting multicomponent VOCs oxidation[J]. Applied Catalysis B: Environmental, 2023, **339**: 123131.[LinkOut]

[27] Zhang N N, Li X M, Guo Y L, et al. Crystal Engineering of TiO_2 for Enhanced Catalytic Oxidation of 1,2-Dichloroethane on a Pt/TiO_2 Catalyst[J]. Environmental Science & Technology, 2023, **57**(17): 7086-7096.
Zhang N N, Li X M, Guo Y L, et al. Crystal engineering of TiO_2 for enhanced catalytic oxidation of 1, 2-dichloroethane on a Pt/TiO_2 catalyst[J]. Environmental Science & Technology, 2023, **57**(17): 7086-7096.[LinkOut]

[28] Roldan R, Beale A, Sanchezsanchez M, et al. Effect of the Impregnation Order on the Nature of Metal Particles of Bi-Functional Pt/Pd-Supported Zeolite Beta Materials and on Their Catalytic Activity for the Hydroisomerization of Alkanes[J]. Journal of Catalysis, 2008, **254**(1): 12-26.
Roldán R, Beale A M, Sánchez-Sánchez M, et al. Effect of the impregnation order on the nature of metal particles of bi-functional Pt/Pd-supported zeolite Beta materials and on their catalytic activity for the hydroisomerization of alkanes[J]. Journal of Catalysis, 2008, **254**(1): 12-26.[LinkOut]

[29] Chen B X, Wang B F, Sun Y H, et al. Plasma-Assisted Surface Interactions of Pt/CeO_2 Catalyst for Enhanced Toluene Catalytic Oxidation[J]. Catalysts, 2018, **9**(1): 2.
Chen B X, Wang B F, Sun Y H, et al. Plasma-assisted surface interactions of Pt/CeO_2 catalyst for enhanced toluene catalytic oxidation[J]. Catalysts, 2019, **9**(1): 2.[LinkOut]

[30] López N, Gómez-Segura J, Marín R P, et al. Mechanism of HCl Oxidation (Deacon Process) over RuO_2[J]. Journal of Catalysis, 2008, **255**(1): 29-39.
López N, Gómez-Segura J, Marín R P, et al. Mechanism of HCl oxidation (deacon process) over RuO_2[J]. Journal of Catalysis,

2008, **255**(1): 29-39.[LinkOut]

[31] Koller V, Lustemberg P G, Spriewald-Luciano A, et al. Critical Step in the HCl Oxidation Reaction over Single-Crystalline CeO_{2-x} (111): Peroxo-Induced Site Change of Strongly Adsorbed Surface Chlorine[J]. ACS Catalysis, 2023, **13**(19): 12994-13007.
Koller V, Lustemberg P G, Spriewald-Luciano A, et al. Critical step in the HCl oxidation reaction over single-crystalline CeO_{2-x} (111): peroxo-induced site change of strongly adsorbed surface chlorine[J]. ACS Catalysis, 2023, **13**(19): 12994-13007.[LinkOut]

[32] Over H, Schomäcker R. What Makes a Good Catalyst for the Deacon Process [J]. ACS Catalysis, 2013, **3**(5): 1034-1046.
Over H, Schomäcker R. What makes a good catalyst for the deacon process? [J]. ACS Catalysis, 2013, 3(5)1034-1046 [LinkOut]

[33] Hua W C, Zhang C H, Guo Y L, et al. An Efficient $Sn_yMn_{1-y}O_x$ Composite Oxide Catalyst for Catalytic Combustion of Vinyl Chloride Emissions[J]. Applied Catalysis B: Environmental, 2019, **255**: 117748.
Hua W C, Zhang C H, Guo Y L, et al. An efficient Sn Mn1-O composite oxide catalyst for catalytic combustion of vinyl chloride emissions[J]. Applied Catalysis B: Environmental, 2019, **255**: 117748.[LinkOut]

[34] Kim W, So J, Choi S, et al. Hierarchical Ga-MFI Catalysts for Propane Dehydrogenation[J]. Chemistry of Materials, 2017, **29** (17): 7213-7222.
Kim W G, So J, Choi S W, et al. Hierarchical Ga-MFI catalysts for propane dehydrogenation[J]. Chemistry of Materials, 2017, 29 (17)7213-7222[LinkOut]

[35] Melo L, Llanos A, Mediavilla M, et al. Acetone Transformation over Pt/H[Al]ZSM5 and Pt/H[Ga]ZSM5 Catalysts Evidences of a Pt-Ga Interaction[J]. Journal of Molecular Catalysis A: Chemical, 2002, **177**(2): 281-287.
Melo L, Llanos A, Mediavilla M, et al. Acetone transformation over Pt/H [Al] ZSM5 and Pt/H [Ga] ZSM5 catalysts Evidences of a Pt - Ga interaction[J]. Journal of Molecular Catalysis A: Chemical, 2002, **177**(2): 281-287.[LinkOut]

[36] Su X F, Wang G L, Bai X F, et al. Synthesis of Nanosized HZSM-5 Zeolites Isomorphously Substituted by Gallium and Their Catalytic Performance in the Aromatization[J]. Chemical Engineering Journal, 2016, **293**: 365-375.
Su X F, Wang G L, Bai X F, et al. Synthesis of nanosized HZSM-5 zeolites isomorphously substituted by gallium and their catalytic performance in the aromatization[J]. Chemical Engineering Journal, 2016, **293**: 365-375.[LinkOut]

[37] Kondo J N, Yamazaki H, Osuga R, et al. Mechanism of Decomposition of Surface Ethoxy Species to Ethene and Acidic OH Groups on H-ZSM-5[J]. Journal of Physical Chemistry Letters, 2015, **6**(12): 2243-2246.
Kondo J N, Yamazaki H, Osuga R, et al. Mechanism of decomposition of surface ethoxy species to ethene and acidic OH groups on H-ZSM-5[J]. The Journal of Physical Chemistry Letters, 2015, **6**(12): 2243-2246.[LinkOut]

[38] Aranzabal A, Romero-Sáez M, Elizundia U, et al. Deactivation of H-Zeolites during Catalytic Oxidation of Trichloroethylene[J]. Journal of Catalysis, 2012, **296**: 165-174.
Aranzabal A, Romero-Sáez M, Elizundia U, et al. Deactivation of H-zeolites during catalytic oxidation of trichloroethylene[J]. Journal of Catalysis, 2012, **296**: 165-174.[LinkOut]

[39] Ying Q J, Liu Y, Li H Y, et al. A Comparative Study of the Dichloromethane Catalytic Combustion over Ruthenium-Based Catalysts: Unveiling the Roles of Acid Types in Dissociative Adsorption and by-Products Formation[J]. Journal of Colloid and Interface Science, 2022, **605**: 537-546.
Ying Q J, Liu Y, Li H Y, et al. A comparative study of the dichloromethane catalytic combustion over ruthenium-based catalysts: Unveiling the roles of acid types in dissociative adsorption and by-products formation[J]. Journal of Colloid and Interface Science, 2022, **605**: 537-546.[LinkOut]

[40] Kang Z H, Zhang X F, Liu H O, et al. Factors Affecting the Formation of Sn-Beta Zeolites by Steam-Assisted Conversion Method[J]. Materials Chemistry and Physics, 2013, **141**(1): 519-529.
Kang Z H, Zhang X F, Liu H O, et al. Factors affecting the formation of Sn-Beta zeolites by steam-assisted conversion method[J]. Materials Chemistry and Physics, 2013, **141**(1): 519-529.[LinkOut]

[41] Wang L, Wu Q Q, Fang T, et al. Boosting Vinyl Chloride Catalytic Combustion and Chlorine Resistance over Ti-Modified Pt/ZrO_2 Catalysts[J]. Separation and Purification Technology, 2025, **372**: 133536.
Wang L, Wu Q Q, Fang T, et al. Boosting vinyl chloride catalytic combustion and chlorine resistance over Ti-modified Pt/ZrO_2 catalysts[J]. Separation and Purification Technology, 2025, **372**: 133536.[LinkOut]

[42] Zhao Y H, Yu Y K, Li J H, et al. Hydrodechlorination under O_2 Promotes Catalytic Oxidation of CVOCs over a Pt/TiO_2 Catalyst at Low Temperature[J]. Chemical Communications, 2025, **61**(24): 4710-4713.
Zhao Y H, Yu Y K, Li J H, et al. Hydrodechlorination under O_2 promotes catalytic oxidation of CVOCs over a Pt/TiO_2 catalyst at low temperature[J]. Chemical Communications, 2025, **61**(24): 4710-4713.[LinkOut]

[43] Liu X L, Zou Y, Li X, et al. Ultralow Doping of Mn Species into Pt Catalyst Enhances the CO Oxidation Performance in the Presence of H_2O and SO_2[J]. ACS Catalysis, 2023, **13**(22): 14580-14597.
Liu X L, Zou Y, Li X, et al. Ultralow doping of Mn species into Pt catalyst enhances the CO oxidation performance in the presence of H_2O and SO_2[J]. ACS Catalysis, 2023, **13**(22): 14580-14597.[LinkOut]

[44] Zhang K Y, Dai L Y, Liu Y X, et al. Insights into the Active Sites of Chlorine-Resistant Pt-Based Bimetallic Catalysts for Benzene Oxidation[J]. Applied Catalysis B: Environmental, 2020, **279**: 119372.
Zhang K Y, Dai L Y, Liu Y X, et al. Insights into the active sites of chlorine-resistant Pt-based bimetallic catalysts for benzene oxidation[J]. Applied Catalysis B: Environmental, 2020, **279**: 119372.[LinkOut]

[45] Xu Z H, Huang G, Yan Z X, et al. Hydroxyapatite-Supported Low-Content Pt Catalysts for Efficient Removal of Formaldehyde at Room Temperature[J]. ACS Omega, 2019, **4**(26): 21998-22007.
Xu Z H, Huang G, Yan Z X, et al. Hydroxyapatite-supported low-content Pt catalysts for efficient removal of formaldehyde at room temperature[J]. ACS Omega, 2019, **4**(26): 21998-22007.[LinkOut]